

OPTICAL PHOTOMETRY AND SPECTROSCOPY OF THE SEYFERT GALAXY SBS 0748+499

J. Torrealba,¹ E. Benítez,¹ A. Franco-Balderas,¹ and V. H. Chavushyan^{1,2}

Received 2005 June 6; accepted 2005 September 13

RESUMEN

Presentamos el primer estudio óptico fotométrico de la galaxia activa SBS 0748+499. Primero mostramos los datos fotométricos en B , V , R e I : las magnitudes totales y los colores $B-V$, $B-R$ y $B-I$; los perfiles de brillo superficial, de color y los perfiles geométricos, poniendo énfasis en la morfología y su relación con las propiedades fotométricas globales de la galaxia. Por tanto, de nuestro estudio de fotometría superficial derivamos el cociente de luminosidades bulbo-disco B/D en las cuatro bandas. Encontramos que la galaxia anfitriona muestra una barra ($a \sim 8$ kpc) y una estructura espiral de bajo brillo superficial, por lo que su clasificación morfológica es SBab. Adicionalmente, presentamos nuevas observaciones espectrofotométricas que muestran claramente que este objeto puede ser clasificado como galaxia Seyfert 1.9. Finalmente, estimamos la masa del agujero negro (M_{BH}) asociado con el núcleo de SBS 0748+499 usando la relación magnitud absoluta en la banda R del bulbo — M_{BH} , y la relación FWHM [O III]₅₀₀₇ — σ_* con un resultado de $M_{BH} = 2.6 \times 10^7 M_\odot$ y $M_{BH} = 8.8 \times 10^7 M_\odot$, respectivamente.

ABSTRACT

We present the first optical photometric study of the active galaxy SBS 0748+499. First, we present B , V , R , and I photometric data: total magnitudes and $B-V$, $B-R$, $B-I$ colors; surface brightness, color and geometric profiles, with emphasis on the morphology and its relation to the global photometric properties of this galaxy. Then, from our surface photometry study we derive the bulge-to-disk luminosity ratio B/D in the four bands. We find that the host galaxy shows a bar ($a \sim 8$ kpc) and a low-brightness spiral structure. The morphological classification for the host galaxy of this AGN is SBab. Additionally, we present new optical spectrophotometric observations that clearly show that the object can be classified as a Seyfert 1.9 galaxy. Finally, we estimate the black hole mass (M_{BH}) associated with the nucleus of SBS 0748+499 using the absolute R -band bulge magnitude — M_{BH} relation, and the FWHM [O III]₅₀₀₇ — σ_* relation. We find that $M_{BH} = 2.6 \times 10^7 M_\odot$ and $M_{BH} = 8.8 \times 10^7 M_\odot$, respectively.

Key Words: GALAXIES: ACTIVE — GALAXIES: SEYFERT — GALAXIES: PHOTOMETRY — GALAXIES: INDIVIDUAL (SBS 0748+499)

1. INTRODUCTION

Since the work of Khachikian & Weedman (1974) Seyfert galaxies were divided into type 1 (Seyfert 1) and type 2 (Seyfert 2) active galactic nuclei (AGN). This classification is based on their optical spectra: Seyfert 1 are those Seyferts that show broad per-

mitted lines with FWHM greater than $\sim 10^3$ km s⁻¹ and also narrow forbidden lines with FWHM $\sim 10^2$ km s⁻¹ while Seyfert 2 show permitted and forbidden narrow lines. Later, Osterbrock (1981) introduced intermediate Seyfert objects that run from 1.2 to 1.9. In particular, Seyfert 1.8 show weak, but readily visible broad H α and H β emission, while Seyfert 1.9 show only broad H α . A new class of Seyfert galaxies showing relatively narrow permitted lines but with line ratios and Fe II emission similar

¹Instituto de Astronomía, Universidad Nacional Autónoma de México, México, D. F., México.

²On sabbatical leave from INAOE, Tonantzintla, Pue., México.

to the Seyfert 1, was introduced by Osterbrock & Pogge (1985). Objects in this class are known as “narrow line Seyfert 1” (NLS1).

Besides their optical spectral characterization, it is also well known that Seyfert galaxies are nearby active galaxies with host galaxies showing large-scale morphologies that resemble those of normal or inactive galaxies (see Taylor et al. 1996; McLure et al. 1999; Bettoni, Falomo, & Fasano 2001). On the other hand, several studies have concluded that the black hole masses are directly proportional to some properties of the galaxy bulge component, e.g., to the mean velocity dispersion of the bulge, the luminosity of the bulge component, etc. We refer the reader to Kormendy & Gebhardt (2001) for a review on this subject. It is also known that only a handful of measurements of black hole masses in Seyfert galaxies have been obtained using essentially reverberation mapping techniques (see Wandel, Peterson, & Malkan 1999; Kaspi et al. 2000; Wandel 2002). However, this method is limited only to Seyfert 1 since according to the unified model the broad line region of Seyfert 2 is hidden from our view. Recently, Boroson (2003) showed that a real correlation exists between the FWHM [O III] and σ_* in QSOs and Seyfert 1 galaxies, although with a large scatter. Nevertheless, it can predict the black hole mass (M_{BH}) to within a factor of 5.

Recently, we have studied the multiwavelength properties of a sample of 25 NLS1 isolated from the Second Byurakan Survey (SBS, see Stepanian et al. 2003). Measuring the line emission ratios of this sample, we discovered that SBS 0748+499 does not show evidences of Fe II emission. It was nevertheless classified as NLS1 by Stepanian et al. (2002), although this is clearly a different type of Seyfert. We also noticed that the dimensions of this object ($\sim 25'' \times 25''$) allow us to study the host galaxy associated to its nucleus with the 1.5 m telescope at OAN-SPM³. Therefore, we decided to study its optical photometric and spectroscopic properties in a separate work. Thus, one of the goals of this paper is to establish its fundamental properties using surface photometry techniques, and also to obtain a more accurate spectroscopic classification of this object using new high signal to noise ratio S/N and moderate resolution spectroscopic observations. A second goal will be the application of the correlation FWHM [O III]– σ_* to estimate the M_{BH} associated to SBS 0748+499, and to compare this result with the

one obtained with a different method (see McLure & Dunlop 2001), based on our estimation of the absolute R -band bulge magnitude M_R for this object.

Finally, we want to point out that the M_{BH} is a fundamental property of AGN because it governs the physics of the central engine. More measurements of black hole masses in nearby galaxies are needed, over the widest possible range of host galaxy types and velocity dispersions, in order to obtain a definitive present-day black hole census (see Barth 2004). Having this in mind, and considering the fact that we obtain the structural parameters of SBS 0748+499 and its morphological classification, along with its optical spectrum, we will be able to give an estimation of M_{BH} that —we assume— inhabits the nucleus of this object, using two different methodologies, under the assumption that they can be applied to intermediate Seyfert galaxies.

The structure of the paper is as follows. The details of the observations and data reduction are given in § 2. We show the results of the aperture photometry in § 3. In section § 4, the geometric and surface brightness profiles of SBS 0748+499 are shown. We present the parameters obtained with the analysis of the profile decomposition that is used to give a morphological classification for the host galaxy. Also, based on our spectroscopical analysis we give the spectral classification of the galaxy in § 5. The parameters obtained in the two later sections are used to give a rough estimation of the black hole mass of the galaxy in § 6. Finally, in section § 7 we present a discussion and our conclusions about this work.

2. OBSERVATIONS

The coordinates of the Seyfert galaxy SBS 0748+499 are: $\alpha = 07^{\text{h}} 51^{\text{m}} 51.9^{\text{s}}$ and $\delta = +49^\circ 48' 51''.6$ (J2000). Based on low-resolution optical spectroscopy, its redshift is $z = 0.0244$.

We have obtained broad band $BVRI$ images of SBS 0748+499 in the Johnson-Cousins system with the 1.5 m telescope at the OAN-SPM. The observations were carried out on November 24th (UT) 2001. We have used a 1024×1024 CCD with a binning of 2×2 pixels, that gives a scale of plate $\sim 0''.51/\text{pix}$. With this configuration we covered an area of $4'.3 \times 4'.3$ in the sky. The integration times were 2400, 1200, 600, and 400 seconds for B , V , R , and I , respectively. We have determined an average seeing of $\sim 2''$ in the four bands using six field stars present in the images. Images in the four filters are uniform, with a sky-brightness of $V = 21.50 \pm 0.01$.

³Observatorio Astronómico Nacional, San Pedro Mártir, Baja California, México.

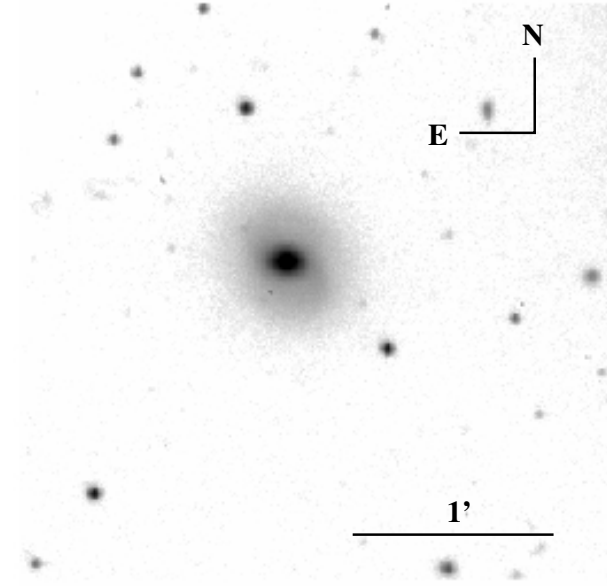


Fig. 1. *B*-band image of SBS 0748+499, barely showing the presence of a low-brightness pseudo-spiral structure. In this paper we assume $H_0 = 75 \text{ km s}^{-1} \text{ Mpc}^{-1}$, therefore, $1'' = 0.47 \text{ kpc}$.

Standard IRAF⁴ procedures for data reduction were used, i.e., bias and dark subtraction, flat-fielding, cosmic-ray removal and sky subtraction to produce the final images. The images were flat-fielded using sky flats taken in each filter at the beginning of the night. Figure 1 shows the *B*-band image of SBS 0748+499.

The photometric calibration was done using three standard stars selected from Landolt's list (Landolt 1992). The equations to transform instrumental magnitudes into standard magnitudes were taken from Franco-Balderas et al. (2003). We observed no significant deviations between the magnitudes we obtain and the standard star magnitudes. The errors in the calibration (quadratic sum of the individual errors) are: $\sigma_B \sim 0.009$, $\sigma_V \sim 0.006$, $\sigma_R \sim 0.008$, and $\sigma_I \sim 0.009$.

Additionally, we have obtained intermediate resolution spectra of SBS 0748+499 with the INAOE's 2.1 m telescope at the GHO⁵ in March 2002, see Figure 2. The Boller & Chivens spectrograph was set in the 4000 – 5700 Å and 5500 – 7200 Å ranges with

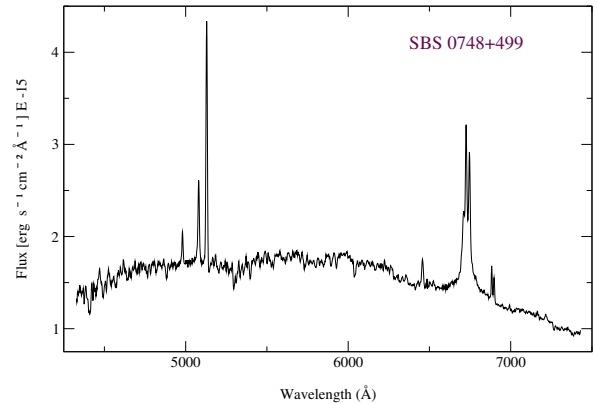


Fig. 2. SBS 0748+499 spectrum obtained with GHO 2.1 m telescope, Cananea, Sonora.

a resolution 1.2 Å/pix , combined with the deployed slit width $2''.5$, that gives an overall resolution of 6 Å FWHM . The S/N ratio was approximately 40 in the continuum near $H\beta$ and $H\alpha$. The spectra were reduced using IRAF routines for long-slit spectroscopy. We also observed standard stars for flux calibration.

3. PHOTOMETRY

We have computed apparent and absolute total magnitudes in *BVRI* bands in two different ways. First, we have used a polygonal aperture chosen interactively with IRAF/APPHOT/POLYPHOT in such a way that it contains the entire galaxy (radius $\sim 60''$). Second, with the IRAF/ISOPHOTE/ELLIPSE, we used an elliptical aperture until $\mu_B = 25 \text{ mag arcsec}^{-2}$ was reached, which corresponds to a semi-major axis length of $19''.7$ (9 kpc), and also up to $50''.6$ (24 kpc) in order to compare these later with the results obtained with the polygonal photometry.

Apparent magnitudes were corrected for atmospheric extinction using the values that we obtained for the OAN-SPM: 0.235 ± 0.010 , 0.147 ± 0.005 , 0.079 ± 0.004 , and 0.053 ± 0.005 for the *B*, *V*, *R*, and *I* filters, respectively. These values are in agreement with those reported by Schuster (1982). Then, these magnitudes were transformed to the standard system. For absolute magnitudes, the correction for Galactic extinction was made using the extinction data presented in NED⁶ from the dust extinction maps of Schlegel, Finkbeiner, & Davis (1998) based on IRAS/DIRBE measurements of diffuse IR emission. We also applied K-corrections interpolated from Frei & Gunn (1994) and inclination corrections from Tully et al. (1998) using the coefficients

⁴IRAF is the Image Reduction and Analysis Facility distributed by the National Optical Astronomy Observatories, which is operated by the Association of Universities for Research in Astronomy (AURA) under agreement with the National Science Foundation (NSF).

⁵Guillermo Haro Observatory at Cananea, Sonora, México.

⁶NASA/IPAC Extragalactic Database.

given by Verheijen (2001). The corrections mentioned above were 0.51, 0.40, 0.34, and 0.26 mag for the B , V , R , and I filters, respectively.

Calculations throughout this paper were done assuming that $H_0 = 75 \text{ km s}^{-1} \text{ Mpc}^{-1}$. We have used $z = 0.0244$ —obtained from our spectroscopic data, this also agrees with the value reported by Stepanian et al. (2002)—and estimated a distance of 98 Mpc for SBS 0748+499. In Table 1 we present the apparent and absolute total magnitudes obtained with the two procedures mentioned above. The estimated accuracies in the apparent magnitudes are ± 0.04 mag in B , ± 0.01 mag in V , ± 0.02 mag in R and I filters. The magnitudes obtained for SBS 0748+499 with polygonal and elliptical apertures at 24 kpc are in very good agreement in all bands, except for the I -band, where a small difference of 0.15 mag was found.

There is only one optical photometric data point for SBS 0748+499 in the literature, that given by Zwicky & Herzog (1966). They found a value of $B = 15.1$ inside an aperture of $18''$ radius. This is consistent with our determination of $B = 15.2$, that was obtained using an elliptical aperture with $a = 19''$ or 9 kpc. Through polygonal and elliptical (9 kpc) apertures we obtained that $M_B = -19.9$. This value is in the range given by Boris et al. (2002) for a sample of Seyfert galaxies (-18.7 to -22.3) with an average value $M_B = -20.7$. From the above estimate, it is clear that SBS 0748+499 is 1.2 mag fainter than the mean value $M_B = -21.1$ reported for normal S0a–Sa UGC sample galaxies (Roberts & Haynes 1994).

Finally, the corrected total colors obtained up to $\mu_B = 25 \text{ mag arcsec}^{-2}$ are: $B - V = 0.84$, $B - R = 1.39$, $V - R = 0.55$, and $V - I = 1.13$. For the elliptical aperture (24 kpc) we obtained $B - V = 0.85$, $B - R = 1.41$, $V - R = 0.55$, and $V - I = 1.13$. For the polygonal aperture the colors are the same except $V - I = 1.24$. These colors are in agreement with the reported average values for Seyfert galaxies given by Chatzichristou (2001).

4. SURFACE PHOTOMETRY

4.1. Geometric Profiles

In order to obtain the radial profiles and geometric parameters of SBS 0748+499, we have used the IRAF/ISOPHOTE/ELLIPSE routine to fit the elliptical contours. This routine is based on the iterative method described by Jedrzejewski (1987). The contours are characterized mainly by: (1) The semi-major axis length (a); (2) the mean intensity (I_m); (3) the ellipticity $\epsilon = 1 - b/a$, where b is the semi-minor axis; (4) the position angle (PA); and (5) the

parameter a_4/a . Note that the a_4/a parameter is a dimensionless measure. It is related to the fourth cosine coefficient of the Fourier series expansion of deviations from a pure ellipse, and gives information about the isophotal shape. So, if $a_4/a > 0$ the isophote is *disky* (pointed ends), if $a_4/a < 0$ the isophote is *boxy* and if $a_4/a = 0$ then we have a perfect ellipse (Bender & Möllenhoff 1987). For more details see Franco-Balderas (2005).

To compute the geometric parameters we have run the routine in free mode giving arbitrary initial values for ϵ , PA and a . The center of each fitted ellipse matched the center of the galaxy obtained with IRAF/DAOFIND routine. Errors in the intensity were obtained from the rms scatter of intensity data along the fitted ellipse, while errors in ϵ and PA are computed by ELLIPSE (Busko 1996). Figure 3 shows that the behavior of ϵ , PA and a_4/a as a function of a is roughly the same in the four filters. Typical errors are $\Delta\epsilon = 0.03$, $\Delta\text{PA} = 8^\circ$, and $\Delta a_4/a = 0.008$.

From the behavior of the geometric parameters we can distinguish basically four different regions:

Region I ($2'' - 4''$): It is dominated mainly by seeing effects, the isophotes are quasi-circular while the PA has a nearly constant value of 87° .

Region II ($4'' - 10''$): From $6'' - 10''$ it can be seen that ϵ grows by 14% and reaches the maximum value in this region, the PA diminishes to 11° , meanwhile $a_4/a \sim 0$. The smooth change in PA is considered as an isophotal twist and could represent a triaxial system according to Wozniak et al. (1995). Elmegreen et al. (1996) performed a study of the isophotal twist in barred galaxies and found that it is related to flat bars. These kinds of bars are present only in early type galaxies (SBa–SBbc). They also found that flat bars are characterized by a continuous increase in the ellipticity. Therefore, this behavior could suggest the existence of a barred structure in this galaxy. However, it is not clearly seen in the brightness profiles.

Region III ($10'' - 18''$): In this region, we observe that $\epsilon \sim 0.24$ and that the PA is systematically decreasing towards 34° . Also, a_4/a is maximum at $14''$, showing that the isophotes are *disky*. This leads us to suggest, accordingly with Elmegreen et al. (1996), that this galaxy has low-brightness spiral-arms embedded in the disk component. This spiral structure is barely visible in our B -band image in Fig. 1.

Region IV ($a > 18''$): The isophotes become circular again fitting the disk's form. At the same time, the PA and a_4/a show larger dispersion due to

TABLE 1
APPARENT AND ABSOLUTE TOTAL MAGNITUDES

Filter	Aperture					
	Polygonal (60''0)		Elliptical (19''7) ^a		Elliptical (50''6) ^a	
	m	M	m	M	m	M
<i>B</i>	15.55	-19.90	15.73	-19.71	15.56	-19.89
<i>V</i>	14.58	-20.75	14.77	-20.56	14.58	-20.75
<i>R</i>	13.96	-21.31	14.16	-21.10	13.97	-21.30
<i>I</i>	13.20	-21.99	13.50	-21.69	13.35	-21.85

^aThe elliptical aperture of 19''7 is characterized by a surface brightness $\mu_B = 25 \text{ mag arcsec}^{-2}$ and corresponds to a semi-major axis length of 9 kpc. Elliptical aperture of 50''6 or 24 kpc contains almost the entire flux of the galaxy.

the diminishing of the intensity of the galaxy, which approaches the sky brightness value.

4.2. Surface Brightness Profile

Surface brightness profiles were obtained by fitting ellipses with a fixed position angle and ellipticity previously determined on the external non-disturbed isophotes. The characteristic values for the fit were: $\epsilon = 0.16 \pm 0.01$ and $\text{PA} = 34^\circ \pm 1^\circ$. The maximum extension for the brightness profiles was set up to 100 pixels or 24 kpc. The optical brightness of the galaxy is totally contained within this radius. Once we obtained the azimuthal mean intensity for each fitted isophote, we transformed it to instrumental surface brightness using the standard procedure described in Franco-Balderas (2005).

In Figure 4 we show the surface brightness profile for the *B*, *V*, *R*, and *I* filters, all corrected for atmospheric extinction and transformed to Landolt's photometric system. We have plotted the surface brightness up to a radius of 39'' (18.6 kpc). This was done because the errors are greater than 1% at this radius. Typical errors in surface brightness were: $\Delta\mu_B = 0.05$, $\Delta\mu_V = 0.02$, $\Delta\mu_R = 0.03$, and $\Delta\mu_I = 0.03$. For clarity, we just show the errors in *B* band. Also in Fig. 4 we observe that $\mu_B = 25 \text{ mag arcsec}^{-2}$ was reached at a semi-major axis length of 19''7; then the estimated semi-minor axis length is 16''5, therefore the inclination angle with respect to the line of sight is $i \approx 33^\circ$ ($i = \cos^{-1} b/a$) for SBS 0748+499.

During the observations, we obtained the characteristic value for the night sky in each band: 22.99 ± 0.05 , 21.50 ± 0.01 , 20.50 ± 0.02 , and 18.68 ± 0.04 for *B*, *V*, *R*, and *I*, respectively. Additionally, Fig-

ure 5 shows the *B*-*V*, *B*-*R*, and *V*-*I* color profiles which have been computed using the values obtained from the surface brightness profile.

4.2.1. Profile Decomposition

The surface brightness profile analysis provides information about the main components of the galaxy. The spiral galaxy bulges are in fact not universally described with an $r^{1/4}$ law (Andreakakis, Peletier, & Balcells 1995). Rather, a continuous range of bulge light profile shapes are now known to exist (see Graham 2001 and references therein; for Seyfert galaxies see Chatzichristou 2001).

The bulge observed in SBS 0748+499 was characterized by an effective radius (r_e) and its corresponding surface brightness (μ_e), a disk with scale length (h) and its extrapolated central surface brightness (μ_0). These four quantities are used to obtain the bulge-to-disk luminosity ratio (B/D) that is useful to establish the morphological classification for the host galaxy of SBS 0748+499.

In order to derive the physical parameters for the components of the galaxy, we have modeled the surface brightness profile with an exponential disk plus a Sérsic $r^{1/n}$ profile (Sérsic 1968) with index n . The Sérsic profile can be written as

$$I(r) = I_e \exp \left\{ -b_n \left[\left(\frac{r}{r_e} \right)^{1/n} - 1 \right] \right\}, \quad (1)$$

where the parameter b_n is determined from the definition of effective radius r_e and I_e is the surface brightness (or half-light) at r_e in intensity units

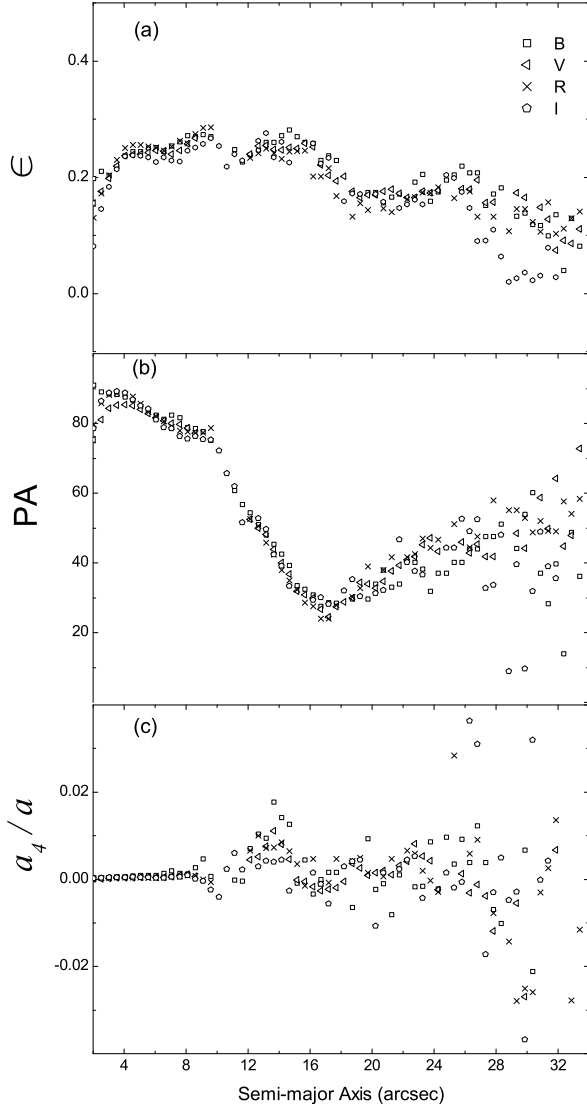


Fig. 3. Geometric profiles: (a) Ellipticity, (b) position angle, and (c) parameter a_4/a versus semi-major axis a .

or μ_e in mag arcsec^{-2} units. From Mazure & Capelato (2002) b_n can be well approximated by $b_n = 1.997n - 0.327$. When $n=4$ the Sérsic model reduces to the $r^{1/4}$ law; for $n=1$ reduces to an exponential profile $I(r) = I_0 \exp\{-r/h\}$, if the central surface brightness of the disk is given by $I_0 = I_e e^{b_n}$ (μ_0 in mag arcsec^{-2} units) and the disk scale length is $h = r_e/b_n^n$.

The decomposition profile was performed as follows. From Fig. 4 we can clearly distinguish an inflection point in the light profile that separates the region where the bulge dominates over the disk. The bulge component is dominant up to $7''$ and the disk component appears roughly linear up to $30''$. Then

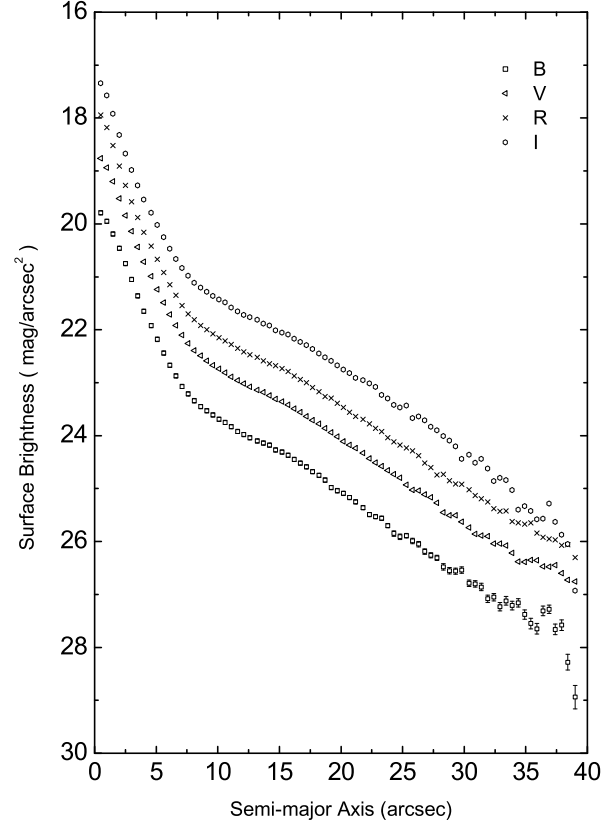


Fig. 4. Surface brightness profiles of the galaxy of SBS 0748+499 in B, V, R , and I filters. The value of $\mu_B = 25 \text{ mag arcsec}^{-2}$ was reached at 9kpc. This isophote was characterized by $\epsilon = 0.16 \pm 0.01$ and $\text{PA} = 34^\circ \pm 1^\circ$.

the profile becomes noisy, but the disk extends over $40''$. Once we have made the distinction between the evident components in the profile, a simultaneous two-component fit was applied until convergence was achieved. That is, at the beginning, we iteratively fitted a function with five parameters: three for the bulge component and, since $n=1$, two for the disk. The χ^2 statistic has been used as an estimator for the quality of the fit. Then, for the geometric profiles and minimization of χ^2 , we found that the best fit for the profile was obtained taking into account an additional component: a bar that can be modeled with a Sérsic profile. The bar component was characterized by a scale radius (r_{bar}) and its corresponding surface brightness (μ_{bar}). The profile fit was performed using an inner cut-off radius of approximately $2''$ to avoid seeing effects. We have chosen for the bulge component the region up to $7''.1$ (3kpc); for the disk we have worked from $7''.1$ up to $30''$ (3–14.5kpc). To describe the full range of the

TABLE 2
GALAXY PARAMETERS OBTAINED FROM THE PROFILE FITS

Filter	μ_e mag arcsec $^{-2}$	r_e (")	μ_0 mag arcsec $^{-2}$	h (")	μ_{bar} mag arcsec $^{-2}$	r_{bar} (")
<i>B</i>	21.05 ± 0.03	2.72 ± 0.04	23.04 ± 0.51	8.84 ± 0.68	24.94 ± 0.51	12.13 ± 0.24
<i>V</i>	20.19 ± 0.02	2.79 ± 0.03	22.28 ± 0.54	9.18 ± 0.55	23.92 ± 0.47	12.38 ± 0.22
<i>R</i>	19.88 ± 0.02	2.95 ± 0.03	21.10 ± 0.09	8.35 ± 0.28	24.04 ± 0.19	12.76 ± 0.26
<i>I</i>	19.24 ± 0.05	2.92 ± 0.03	20.52 ± 0.36	8.35 ± 0.82	23.09 ± 0.60	13.52 ± 0.45

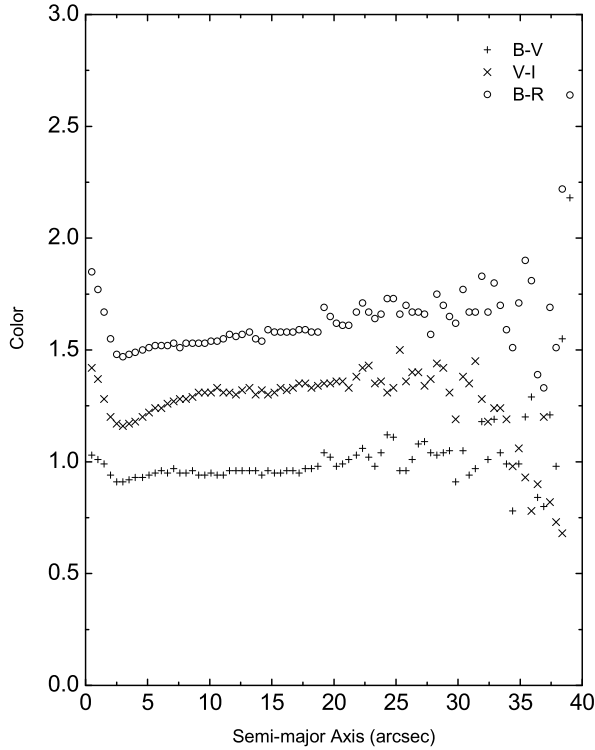


Fig. 5. The behavior of the colors ($B - V$), ($V - I$), and ($B - R$) of SBS 0748+499 is shown in this plot. It can clearly be observed that the center is the reddest part, and that colors appear flatter in the region between $2''$ – $20''$ (1–9.5 kpc). The dispersion is larger in the external parts of the galaxy due to the increasing contribution of the sky.

intensity profile we have added the contribution of the three components, in other words:

$$I(r) = I(r)_{bulge} + I(r)_{disk} + I(r)_{bar}. \quad (2)$$

The decomposition of the surface brightness profile was done for B , V , R , and I bands. Our best fit parameters for each band are given in Table 2 and

TABLE 3
SÉRSIC INDEX^a AND BULGE-DISK
LUMINOSITY RATIO

Filter	Sérsic n (bulge)	Sérsic n (bar)	B/D
<i>B</i>	0.77 ± 0.04	0.33 ± 0.12	1.00 ± 0.78
<i>V</i>	0.78 ± 0.03	0.36 ± 0.11	1.09 ± 0.83
<i>R</i>	0.58 ± 0.02	0.36 ± 0.05	0.58 ± 0.10
<i>I</i>	0.66 ± 0.05	0.33 ± 0.20	0.63 ± 0.37

^a The Sérsic index applied for the disk component in the model profile was fixed to $n = 1$, an exponential disk.

we show in Table 3 the index n for the bulge and bar components. The decomposition profile for R band is shown in Figure 6.

4.2.2. Bulge and Disk Parameters

The total luminosity described by a Sérsic $r^{1/n}$ profile is given by Graham et al. (1996) as

$$L_{tot} = \int_0^{\infty} I(r) 2\pi r dr = \frac{n 2\pi r_e^2 I_e e^{b_n}}{b_n^{2n}} \Gamma(2n), \quad (3)$$

where Γ is the Gamma function and b_n is the parameter defined in previous section. Therefore, the bulge-to disk luminosity ratio is given by the expression:

$$\frac{B}{D} = \frac{n_b e^{b_n}}{b^{2n_b}} \left(\frac{r_e^2}{h^2} \right) \left(\frac{I_e}{I_0} \right) \Gamma(2n), \quad (4)$$

where the B and D are the bulge and disk luminosities of the galaxy; the index n_b is the Sérsic index for the bulge; r_e , I_e , h , and I_0 are the parameters related to the bulge and the disk, respectively.

The integral of intensity shown in Eq. (3) only has an analytical expression for integer values of $n \geq 1$ and in some particular cases where $0 \leq n \leq 1$

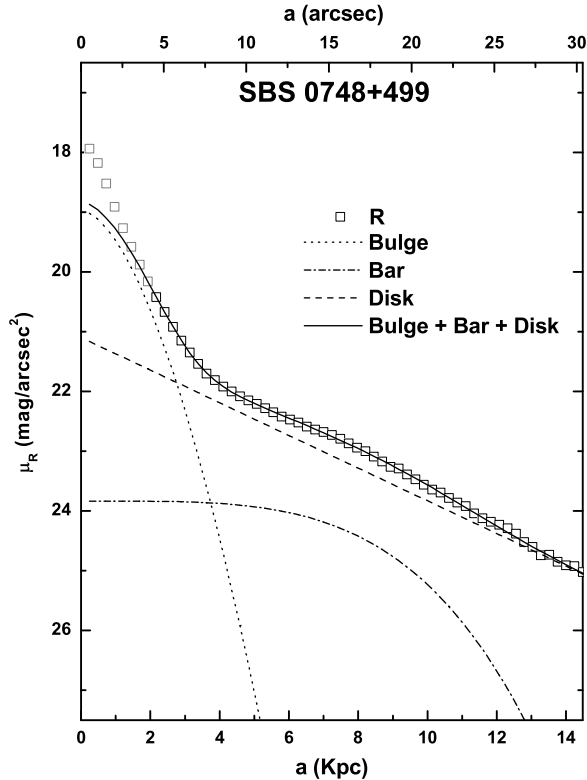


Fig. 6. Profile decomposition for SBS 0748+499 in the R band. The light profile of this galaxy is remarkably well described by three components: a bulge and a bar modeled with a Sérsic profile and an exponential disk. In the center of the profile the model differs from the observations because an inner cutoff of $2''$ was applied during the decomposition procedure.

(e.g., 0.2, 0.4). Table 3 shows that the bulge component index n varies between 0.77 in B and 0.58 in the R band. For this reason, to estimate B/D we considered the bulge luminosity separately doing an interpolation for the corresponding values of n . This interpolation was obtained from the values where Eq. (3) has an analytical solution. The values obtained for the ratio B/D are shown in Table 3.

For a sample of Seyfert galaxies Chatzichristou (2001) obtained a wide range of values for μ_e , with average values of 17.64 for Seyfert 1 and 18.77 for Seyfert 2, while for r_e reports values of 1.35 and 1.06, respectively. Also, this author has found that typical values for both types of Seyfert galaxies are $h \sim 1-10$ kpc and $\mu_0 \sim 18-24$ mag arcsec $^{-2}$. Thus, our estimated values of μ_e , μ_0 , and h are in agreement with the values reported by Chatzichristou for Seyfert galaxies.

Using the classification scheme established for a sample of field galaxies from *HST* Medium Deep

TABLE 4
SPECTROSCOPIC DATA

Ion	λ (\AA)	Flux (10^{-15} erg s $^{-1}$ cm $^{-2}$)	EW (\AA)
[S II]	6731	2.7	2.0
[S II]	6716	1.9	1.4
[N II]	6583	11.7	7.6
H α broad	6567	22.2	14.4
H α narrow	6563	12.8	8.3
[N II]	6548	3.9	2.5
[O I]	6300	3.7	2.5
[O III]	5007	23.7	14.0
[O III]	4959	8.0	4.6
H β	4861	3.2	1.9

^aNote: All parameters are given in the rest frame.

Survey (Schmidtke et al. 1997), we can see that the obtained value $B/D = 0.58$ in the R band for SBS 0748+499 falls in the range $0.5 < B/D < 1.7$, so this object can be classified as an intermediate type galaxy (SBab). However, the typical spiral structure is not clearly present in this object.

5. SPECTRAL CLASSIFICATION

Line fitting analysis for the optical spectra of SBS 0748+499 was done in terms of Gaussian components (Véron, Véron-Cetty, & Zuiderwijk 1981). Also, the width and redshifts of each narrow line component were fixed to the same value. For the fitting, we assumed that the intensity ratios of [N II] $\lambda\lambda 6548, 6583$ and [O III] $\lambda\lambda 4959, 5007$ lines were equal to 3 and 2.96, respectively (Osterbrock 1989). For H α and [N II], we have done the fitting using Gaussian components (three narrow and one broad) in the centroid of H α . For H β and [O III] $\lambda\lambda 4959, 5007$ lines, we used three narrow Gaussian components. The local continuum in the H β and H α spectral ranges was approximated inside the 4500–5500 \AA and 6000–7000 \AA regions, respectively. Results are given in Table 4 and in Figures 7 and 8. A least-squares fit was performed using the IRAF/GUIAPPS/SPECTOOL package, and is shown in Fig. 7. In order to classify SBS 0748+499, we used the diagnostic diagrams $\log([\text{O I}]\lambda 6300/\text{H}\alpha)$, $\log([\text{N II}]\lambda 6583/\text{H}\alpha)$, and $\log([\text{S II}]\lambda\lambda 6717+6731/\text{H}\alpha)$ versus $\log([\text{O III}]\lambda 5007/\text{H}\beta)$ (Veilleux & Osterbrock 1987).

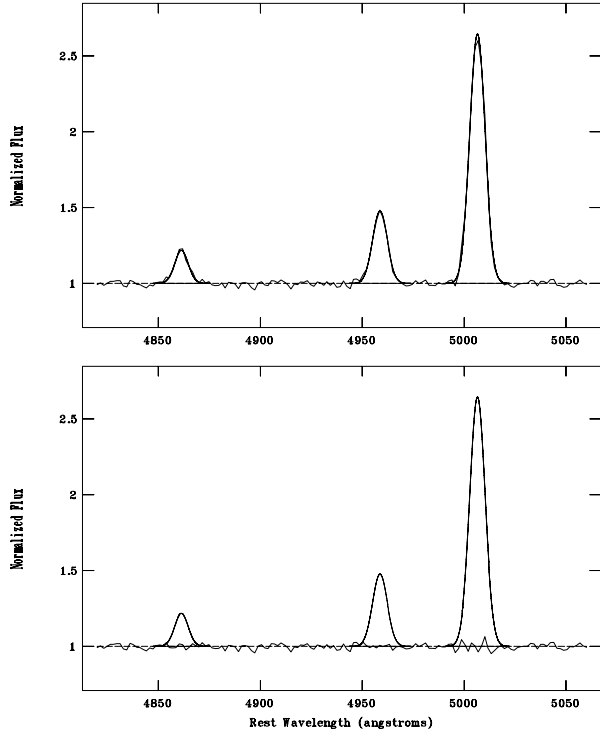


Fig. 7. De-redshifted smoothed blue normalized spectra of SBS 0748+499. The upper panel shows the best fit with three narrow Gaussian components profiles for H β and [O III]. The bottom panel shows individual Gaussian components and the differences between the data and the best fit, i.e., the residuals.

On all the diagnostic diagrams the values for the logarithms [O I] λ 6300/H α = -0.54 , [N II] λ 6583/H α = -0.04 , [S II] λ λ 6717+6731/H α = -0.44 , and [O III] λ 5007/H β = -0.87 locate the object inside the AGN region.

Thus, according to Osterbrock (1981), SBS 0748+499 can be classified as Seyfert 1.9, mainly because we can only see the broad H α component with a FWHM = 1700 km s $^{-1}$. The narrow lines that appear in Table 4 all have a FWHM = 450 km s $^{-1}$.

6. BLACK HOLE MASS ESTIMATION

We have used two different methods to give an estimation of the black hole mass of SBS 0748+499. The first one is based on the absolute R -band magnitude of the bulge component obtained from the photometric data, i.e., from the host galaxy. The second one is based on an estimation of the stellar velocity dispersion of the bulge which was derived indirectly from our spectroscopic data. The first method is

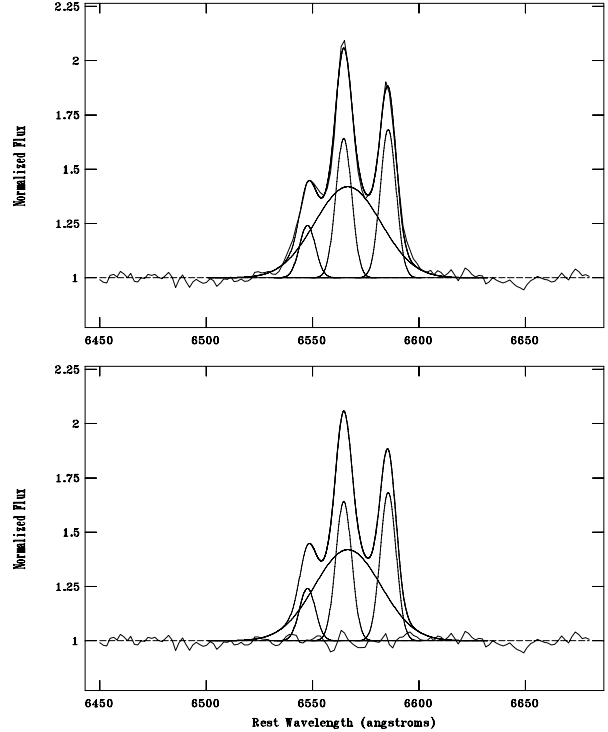


Fig. 8. De-redshifted smoothed red normalized spectra of SBS 0748+499. The upper panel shows the best fit using three narrow plus one broad Gaussian components profiles for H α and [N II]. The bottom panel shows individual Gaussian components and the differences between the data and the best fit.

based on the application of the relation between absolute R -band magnitude M_R and M_{BH} given by McLure & Dunlop (2002). We have recalculated this relation for our cosmology as:

$$\log(M_{BH}/M_{\odot}) = -0.50(\pm 0.02)M_R - 2.52(\pm 0.48). \quad (5)$$

From the luminosity of the bulge component in R -band $L_R = (5.17 \pm 0.21) \times 10^9 L_{\odot}$ we have $M_R = -19.86 \pm 0.05$, and we obtain $\log M_{BH}/M_{\odot} = 7.41 \pm 0.48$.

The second method needs an indirect inference of the bulge stellar velocity dispersion. The brightness of the nuclear part of SBS 0748+499 does not allow us to detect the absorption lines of CaT in the spectrum (lines commonly used to estimate σ_* , e.g., Onken et al. 2004). Therefore, we decided to use the relation found by Nelson (2000): $\sigma_* = \text{FWHM}[\text{O III}]_{5007}/2.35$, on the assumption that for this galaxy the forbidden line kinematics is dominated by virial motions in the host galaxy bulge. Also,

this author found the following relation for the black hole mass:

$$\log(M_{BH}/M_{\odot}) = 3.7(\pm 0.7) \log \sigma_{*} - 0.5(\pm 0.1). \quad (6)$$

This method has been investigated later by Boroson (2003) using the Sloan Digital Sky Survey Early Data Release spectra of 107 low redshift quasars and Seyfert 1 galaxies. He confirms the existence of the relation σ_{*} versus FWHM [O III]₅₀₀₇ and claims that this relation can predict the black hole mass in active galaxies to within a factor of 5. So, measuring the FWHM of the narrow line [O III]₅₀₀₇ = 450 ± 14 km s⁻¹ from our spectrum (see § 5) we obtain $\sigma_{*} = (191 \pm 6)$ km s⁻¹ which yields a value for the mass of the black hole of $\log M_{BH}/M_{\odot} = 7.94 \pm 1.6$.

The values found with the methods described above differ by a factor of 3, and the photometric method developed by McLure & Dunlop (2002) provides an estimation with a lower dispersion.

7. DISCUSSION AND CONCLUSIONS

From the *B*-band image in Fig. 1 and also from the surface brightness profiles (see Fig. 4) we can clearly distinguish a bulge and a disk component, as well as a bar-like structure in the host galaxy of SBS 0748+499. This is important since bar-induced inflows are frequently cited mechanisms for funnelling some gas to the nucleus, thereby temporarily activating an otherwise normal galaxy. Additionally, from the geometric profiles we infer the presence of low surface brightness spiral structure. In § 4.2.2 we obtained a value of 0.58 for the bulge-to-disk luminosity ratio in *R* band, which suggests that SBS 0748+499 is an SBab type. We can barely appreciate the spiral-arm structure in Fig. 1; however we could not distinguish any star forming regions, typically expected in Sab type galaxies. On the other hand, we have done a comparison between the color $B - V = 0.84$ obtained in § 3 and the mean value reported for galaxies S0a, Sa $B - V = 0.78$ by Roberts & Haynes (1994). We found that SBS 0748+499 is only 0.06 mag redder than these early-type galaxies. This could indicate that SBS 0748+499 is earlier than a Sb galaxy. Gronwall, Sarajedini, & Salzer (2002) found that Seyfert 2 and LINERS are preferentially found in redder hosts $B - V = 0.92$ while Seyfert 1 hosts typically have bluer colors $B - V = 0.70$. We have shown in § 5 that SBS 0748+499 is a Seyfert 1.9, so the color range found for it will fill the gap between Seyfert 1 and Seyfert 2, supporting the result that it is an intermediate Seyfert type galaxy. Additionally, we have estimated that the optical luminosity of SBS 0748+499 is $L_B = 6.6 \times 10^{42}$ erg s⁻¹

($M_B = -19.9$), a typical value for Seyfert galaxies Schmidt & Green (1983).

From its optical spectrum, it is clear that SBS 0748+499 does not show the H β broad component; therefore the only way to estimate M_{BH} is to use the two different correlations described in the last section. Our main hypothesis for using the FWHM [O III]₅₀₀₇ (i.e., the NLR in intermediate Seyfert) is based on the fact that this quantity should be related to the stellar velocity dispersion of the host galaxy, and therefore to the M_{BH} as it has been previously found. On the other hand, the M_R bulge in this work was obtained using the best fitted parameters excluding the innermost 2'' region.

The relation that involves M_R bulge provides an estimation of the M_{BH} that is within the uncertainties obtained with the FWHM [O III]₅₀₀₇ - σ_{*} relation. At this point, we consider that both estimates are in good agreement, and that the photometric method provides lower uncertainties. Also, it is interesting to note that both correlations are calibrated and based on Type 1 AGN (Seyfert 1 and QSO), and also that McLure & Dunlop (2002) have demonstrated that the M_R bulge - M_{BH} correlation is also valid for quiescent galaxies.

SBS 0748+499 is a nearby AGN, so it can be studied in more detail. In future work, it would be worthy to study a well defined sample of nearby intermediate Seyfert galaxies in order to estimate the σ_{*} and see if, in particular, the so-called σ_{*} - M_{BH} scales in the same form as it does for Seyfert 1 galaxies. In particular, new observations with better resolution are needed to establish the nuclear morphology in the innermost arcsecond region of SBS 0748+499.

The authors want to acknowledge an anonymous referee for very useful comments and suggestions, which helped to improve this work. We also thank Dr. W. Lee who carefully read the final version of the typescript. J. T. acknowledges financial support from grant IN-118601 (PAPIIT-UNAM) scholarship. E. B. acknowledges grants IN-112305 (PAPIIT-UNAM) and CONACyT No. 40096-F for the support given to this research. V. Ch. acknowledges CONACyT basic research grant No. 39560-F. We also acknowledge the OAN-SPM and OAGH staff for their support during the observations. This research has made use of the NASA/IPAC Extragalactic Database (NED) which is operated by the Jet Propulsion Laboratory, California Institute of Technology, under contract with the National Aeronautics and Space Administration.

REFERENCES

- Andrekaakis, Y. C., Peletier, R. F., & Balcells, M. 1995, *MNRAS*, 275, 874
- Barth, A. 2004, in *Coevolution of Black Holes and Galaxies*, ed. L. Ho, Carnegie Observatories Astrophysics Series (Cambridge: Cambridge Univ. Press), Vol. 1, 21
- Bender, R., & Möllenhoff, C. 1987, *A&A*, 177, 71
- Bettoni, D., Falomo, R., & Fasano, G. 2001, *A&A*, 380, 471
- Boris, N. V., Donzelli, C. J., Pastoriza, M. G., et al. 2002, *A&A*, 384, 780
- Boroson, T. A. 2003, *ApJ*, 585, 647
- Busko, I. 1996, *PASP Conf. Series*, 101, 139
- Chatzichristou, E. 2001, *ApJ*, 556, 653
- Elmegreen, D. M., Elmegreen, B. G., Chromey, F. R., et al. 1996, *AJ*, 111, 1880
- Franco-Balderas, A., Hernández-Toledo, H. M., Dultzin-Hacyan, D., & García-Ruiz, G. 2003, *A&A*, 406, 415
- Franco-Balderas, A. 2005, Ph.D. thesis, UNAM, in preparation
- Frei, Z., & Gunn, J. E. 1994, *AJ*, 108, 1476
- Graham, A. W. 2001, *AJ*, 121, 820
- Graham, A. W., Lauer, T., Colless, M. M., & Postman, M. 1996, *ApJ*, 465, 534
- Gronwall, C., Sarajedini, V. L., & Salzer, J. J. 2002, in *ASP Conf. Ser.*, Vol. 284, *AGN Surveys*, eds. R. F. Green, E. Y. Khachikian, & D. B. Sanders (San Francisco: ASP), 43
- Jedrzejewski, R. I. 1987, *MNRAS*, 226, 747
- Kaspi, S., Smith, P. S., Netzer, H., et al. 2000, *ApJ*, 533, 631
- Kormendy, J., & Gebhardt, K. 2001, *AIP Conf. Proceedings* 586, 20th Texas Symposium, eds. J. C. Wheeler & H. Martel (Austin, TX: American Institute of Physics)
- Khachikian, E. Y., & Weedman, P. W. 1974, *ApJ*, 192, 581
- Landolt, A. U. 1992, *AJ*, 104, 340
- McLure, R. J., & Dunlop, J. S. 2002, *MNRAS*, 331, 795
 _____ 2001, *MNRAS*, 327, 199
- McLure, R. J., Kukula, M. J., Dunlop, J. S., et al. 1999, *MNRAS*, 308, 377
- Mazure, A., & Capelato, H. V. 2002, *A&A*, 383, 384
- Nelson, C. H. 2000, *ApJ*, 544, L91
- Onken, C. A., Ferrarese, L., Merritt, D., et al. 2004, *ApJ*, 615, 645
- Osterbrock, D. E. 1981, *ApJ*, 249, 462
 _____ 1989, *Astrophysics of Gaseous Nebulae and Active Galactic Nuclei* (Mill Valley, CA: Univ. Sci.)
- Osterbrock, D. E., & Pogge, R. W. 1985, *ApJ*, 297, 166
- Roberts, M. S., & Haynes, M. P. 1994, *ARA&A*, 32, 115
- Schmidtke, P. C., Windhorst, R. A., Mutz, S. B., et al. 1997, *AJ*, 113, 569
- Schlegel, D. J., Finkbeiner, D. P. & Davis, M. 1998, *ApJ*, 500, 525
- Schmidt, M., & Green, R. F. 1983, *ApJ*, 269, 352
- Schuster, W. 1982, *RevMexAA*, 5, 149
- Sérsic, J. L. 1968, *Atlas de Galaxias Australes* (Córdoba: Obs. Astronómico)
- Stepanian, J. A., Benítez, E., Krongold, Y., et al. 2003, *ApJ*, 588, 746
- Stepanian, J. A., Chavushyan, V. H., Carrasco, L., et al. 2002, *AJ*, 124, 1283
- Taylor, G. L., Dunlop, J. S., Hughes, D. H., & Robson, E. I. 1996, *MNRAS*, 283, 930
- Tully, R. B., Pierce, M. J., Huang, Jia-Sheng, et al. 1998, *AJ*, 115, 2264
- Veilleux, S., & Osterbrock, D. E. 1987, *ApJS*, 63, 295
- Véron, P., Véron-Cetty, M.-P., & Zuiderwijk, E. K. 1981, *A&A*, 102, 116
- Verheijen, M. A. W. 2001, *ApJ*, 563, 694
- Wandel, A. 2002, *ApJ*, 565, 762
- Wandel, A., Peterson, B. M., & Malkan, M. A. 1999, *ApJ*, 526, 579
- Wozniak, H., Friedli, D., Martinet, L., Martin, P., & Bratschi, P. 1995, *A&AS*, 111, 115
- Zwicky, F., & Herzog, E. 1966, *Catalogue of Galaxies and Clusters of Galaxies*, Vol. III, (Pasadena: CALTECH)

Erika Benítez, Alfredo Franco-Balderas, and Janet Torrealba: Instituto de Astronomía, UNAM, Apdo. Postal 70-264, 04510 México D. F., México (erika,alfred,cjanet@astroscu.unam.mx).

Vahram H. Chavushyan: Instituto Nacional de Astrofísica, Óptica y Electrónica (INAOE), Apartado Postal 51 and 216, 72000 Puebla, Pue., México (vahram@astroscu.unam.mx; vahram@inaoep.mx).